*J. Fluid Mech.* (1975), *vol.* 71, *part* 4, *pp.* 785–800
*Printed in Great Britain*



# Cross-wire anemometry in high intensity turbulence

By NARINDER K. TUTU AND RENE CHEVRAY
Department of Mechanics, State University of New York, Stony Brook

(Received 27 January 1975)

An analysis of the response of an X-probe which takes into account the axial sensitivity $k$, the effect of the $w$ component of velocity and the effective rectification by the hot wire is presented. Owing to rectification points in the measured $u, v$ 'phase plane' are confined within a certain sector, thus leading to distortions in the measured joint probability density functions. Numerical computations show that high turbulence intensities lead to large errors in second-order moments measured by cross-wire probes; for instance, the error in the measured correlation (over and above that due to $k$) can be as high as 28 % when the turbulence intensity is 35 %.

## 1. Introduction

It is well known that measurements of components of the turbulent stress tensor in high intensity turbulent flows like free turbulent jets, mixing layers etc. are very difficult and can lead to significant errors. This is usually thought of as a consequence of truncating the series expansion of the hot-wire response equation

$$U_{\text{eff}} = \{U^2_{\text{normal}} + k^2 U^2_{\text{axial}}\}^{\frac{1}{2}}, \tag{1.1}$$

where $U_{\text{eff}}$ is the instantaneous effective cooling velocity, $U_{\text{normal}}$ and $U_{\text{axial}}$ are the components of the velocity vector normal and parallel to the hot wire, respectively, and $k$ is the axial sensitivity of the hot wire. While Champagne, Sleicher & Wehrmann (1967) have clearly demonstrated the dependence of $k$ on the length-to-diameter ratio $l/d$ of the hot wire, in addition to determining its value as a function of $l/d$, Champagne & Sleicher (1967) have given the corrections (valid for small turbulence intensities) to be applied to measurements owing to the influence of $k$. An important source of error, however, is the resultant rectification of the velocity signal by the hot wire, the hot wire being sensitive only to the magnitude of the effective cooling velocity. Rectification occurs whenever the component of velocity normal to the hot wire crosses zero. Although for a hot wire held normal to the flow this will obviously happen only during flow reversals, this is not so for cross-wires which are inclined to the flow. Since $U_{\text{eff}}$ is always positive, the errors due to rectification arise not because of truncation of the series expansion of the right-hand side of (1.1), but because during signal processing the modulus sign implicit on the right-hand side of (1.1) is ignored. Thus (1.1) should really be written as $U_{\text{eff}} = |\{U^2_{\text{normal}} + k^2 U^2_{\text{axial}}\}^{\frac{1}{2}}|$. To see this more clearly consider a hot

wire normal to the mean flow. Let $u$, $v$ and $w$ be the three components of the instantaneous velocity vector. Then let

$$u = U + u', \quad v = V + v', \quad w = W + w',$$

where $U$, $V$ and $W$ are the mean velocities and $u'$, $v'$ and $w'$ are the fluctuations. If $v = w = 0$ and the hot wire is held normal to the $u$ direction, then in general

$$U_{\text{eff}} = \{(U+u')^2\}^{\frac{1}{2}} = |U+u'| \neq U+u',$$

$$\overline{U}_{\text{eff}} = \overline{|U+u'|} \neq U,$$

$$\overline{(U_{\text{eff}} - \overline{U}_{\text{eff}})^2} = \overline{(|U+u'| - \overline{|U+u'|})^2} \neq \overline{u'^2}.$$

This rectification can be observed easily by studying the bounds of the phase diagram generated by signals from two orthogonal hot wires (an X-probe). Figures 1 (*a*), (*b*) and (*c*) (plate 1) show the phase diagrams generated by an X-probe at the centre-line, point of maximum shear and approximate half-intermittency point in an axisymmetric jet 15 diameters downstream. The co-ordinates in these figures are the linearized outputs from two hot wires held at $\pm 45°$ to the mean flow direction. These photographs were obtained by operating a d.c. coupled oscilloscope in the storage mode for about 3 min. As can be seen, points in the phase plane are bounded by two straight lines. This boundary shows that the linearized output voltage for one wire has reached a value indicating that the flow is parallel to that wire (putting $U_{\text{normal}} = 0$ in (1.1) we obtain $U_{\text{eff}} = kU_{\text{axial}}$); for the case $k = 0$, that voltage being zero, the angle between the two straight-line boundaries will be 90°.

Obviously the information lost owing to rectification can never be recovered; however, since the square of a rectified signal is identical to the square of the signal itself, by using a single wire held at different angles and processing the squared signals, sufficient information would be obtained so that certain moments could be measured. This was partially done by Rodi (1971), though for a different reason, namely to avoid the series expansion of the square root. Unfortunately, however, he assumed $V = 0$ in the formulation, which although $V$ is usually very small, can, as will be shown later, lead to large errors in the measured correlation $\overline{uv}$. Consider a hot wire in the $u$, $v$ plane as shown in figure 2. Let $\alpha$ be the angle between the normal (in the $u$, $v$ plane) to the wire and the $u$ axis. Then the effective cooling velocity $U_{\text{eff}}$ is given by

$$U_{\text{eff}}^2 = [(U+u')\cos\alpha + (V+v')\sin\alpha]^2 + w^2 + k^2[(u'+U)\sin\alpha - (V+v')\cos\alpha]^2. \tag{1.2}$$

The so-called pitch factor $h$, which would have resulted in a term $h^2w^2$ instead of $w^2$ in the above equation, is assumed to be unity. This is because it can be very sensitive to the prong and probe configuration, and since the later computations involve numerical values one choice is as good as another. It is easy to see that an average of (1.2) will result in six unknown moments: $U$, $V$, $\overline{u'^2}$, $\overline{v'^2}$, $\overline{w^2}$ and $\overline{u'v'}$. Thus accurate measurement of these quantities without errors due to rectification and truncation will require six choices of $\alpha$ and solution of six simultaneous equations.

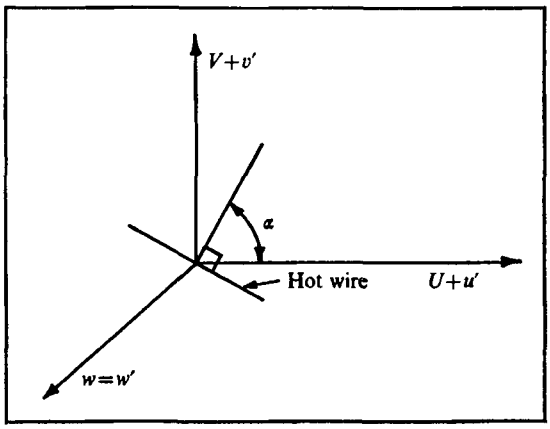


FIGURE 2. Definition sketch of hot wire in $u$, $v$ plane.

Most of the $\overline{u'v'}$ correlation measurements published in the literature have been made with an X-probe in the conventional way. Wygnanski & Fiedler (1969), who made measurements in an axisymmetric jet, did not apply any corrections resulting from higher-order terms. Although Heskestad (1965) did correct his measurements by including higher-order terms, these involved assumptions about the behaviour of higher-order moments. More important, however, these corrections did not take rectification into account. Recently Eckelmann (1974) has made measurements in the wall region of a turbulent channel flow, where the turbulent intensity can be as high as 34 %. He also neglected the effects of rectification and higher-order terms. Thus there is motivation for finding the order-of-magnitude of errors in such measurements due to the combined effects of rectification and truncation. There is another important reason. Probability-density-function (p.d.f.) measurements require instantaneous signals directly proportional to the variables of interest. Although it is theoretically possible to get, say, simultaneous instantaneous signals for $u$ and $v$ without the effects of rectification and distortion due to axial cooling and the presence of the $w$ component, this is not practical. It would require a special probe with seven hot wires, all mounted at different angles. Treating $U$, $u'$, $v = V+v'$ and $w$ as effective variables, (1.2) results in a linear equation in the following seven unknowns: $U^2$, $u'^2$, $u'U$, $v^2$, $vU$, $vu'$ and $w^2$; so $u$ and $v$ could in principle be obtained exactly using a seven-wire probe. The prong and inter-wire interference would, of course, be overwhelming in such a case. Thus the only recourse for measurement of the joint p.d.f. of $u$ and $v$ or the marginal p.d.f. of $v$ is a conventional X-probe. It is therefore important to see how the joint p.d.f. surface in the $u$, $v$ plane is distorted owing to rectification, the effects of axial cooling and $w$, so that care may be taken in interpreting the p.d.f. data.

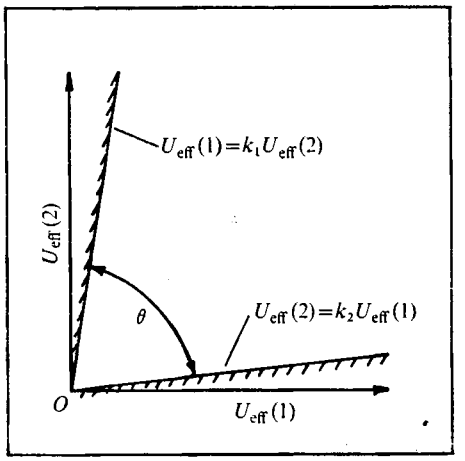


FIGURE 3. Bounds in the 'phase diagram' for signals from two orthogonal hot wires.

## 2. Analysis

### 2.1. *The equations for bounds in the 'phase plane' of an* X*-probe*

It will be assumed throughout that linearized hot-wire anemometers are being used; then there is a linear relationship between the linearizer voltage and the effective cooling velocity.

Consider an X-probe with the two wires in the $x$, $y$ plane and perpendicular to each other. Choose the co-ordinate axes $x$ and $y$ along wires 1 and 2, respectively, the $z$ axis then being normal to the $x$, $y$ plane. Let $Q_x$, $Q_y$ and $Q_z$ be the components of the instantaneous velocity vector along the $x$, $y$ and $z$ axes. Then the effective cooling velocities $U_{\text{eff}}(1)$ and $U_{\text{eff}}(2)$ for the two wires are given by

$$U^2_{\text{eff}}(1) = Q_y^2 + Q_z^2 + k_1^2 Q_x^2, \tag{2.1}$$

$$U^2_{\text{eff}}(2) = Q_x^2 + Q_z^2 + k_2^2 Q_y^2. \tag{2.2}$$

Equations (2.1) and (2.2) can be rewritten as

$$U^2_{\text{eff}}(1) = k_1^2 U^2_{\text{eff}}(2) + (1-k_1^2)(Q_z^2 + k_2^2 Q_y^2) + (1-k_2^2) Q_y^2, \tag{2.3}$$

$$U^2_{\text{eff}}(2) = k_2^2 U^2_{\text{eff}}(1) + (1-k_2^2)(Q_z^2 + k_1^2 Q_x^2) + (1-k_1^2) Q_x^2. \tag{2.4}$$

Since $k_1$, $k_2 < 1$, (2.3) and (2.4) imply that

$$U_{\text{eff}}(1) \geqslant k_1 U_{\text{eff}}(2), \quad U_{\text{eff}}(2) \geqslant k_2 U_{\text{eff}}(1). \tag{2.5}$$

From (2.1) and (2.2), we have

$$U_{\text{eff}}(1),\ U_{\text{eff}}(2) \geqslant 0. \tag{2.6}$$

The condition (2.6) restricts points in the $U_{\text{eff}}(1)$, $U_{\text{eff}}(2)$ phase plane to the first quadrant, whereas (2.5) restricts them to the sector shown in figure 3. The included angle $\theta$ of the sector is then given by

$$\theta = \tfrac{1}{2}\pi - (\tan^{-1} k_1 + \tan^{-1} k_2), \tag{2.7}$$

which is equal to $\frac{1}{2}\pi$ when $k_1 = k_2 = 0$. Henceforth, for simplicity it will be assumed that $k_1 = k_2 = k$.

The average value of $\theta = 72°$ was determined from several photographs similar to those in figure 1. This corresponds to $k = 0{\cdot}16$ for our hot wires. This agrees very well with the estimated value of $0{\cdot}15 \pm 0{\cdot}04$ given by Champagne *et al.* (1967) for our probe ($l/d = 300$). However, it should be noted that the $k$ thus found need not necessarily be the same as that determined from the results of Champagne *et al.* Indeed, from (2.1)–(2.5) it is clear that a point in the phase diagram lies on the bound only when the instantaneous velocity vector is along one of the hot wires, which corresponds to an instantaneous yaw angle $\alpha = 90°$. Considering $k$ to be a function of $\alpha$, it is clear that the $k$ used in (2.5) and (2.7) corresponds to $\alpha = \frac{1}{2}\pi$. Although Champagne *et al.* have found no variation of $k$ for $-60° < \alpha < 60°$, it obviously does not follow that it is a constant outside this domain as well. Our preliminary rough measurements indicate that $k(90°)$ and, say, $k(45°)$ can be very different. For two wires with different ratios $l/d$ (100 and 700), while the ratio of the $k$'s for $\alpha = 20°$ was found to be 2 it was almost unity for $\alpha = 90°$. Furthermore, $k(90°)$ for the above two wires was approximately the same as it was for $l/d = 300$. Thus it seems that $k(90°)$ is insensitive to $l/d$; so one should not be surprised if the experimentally determined $\theta$ does not correspond to the $k$ estimated from the results of Champagne *et al.* If $k(90°) = k(45°)$, which our results indicate to be true for wires with $l/d$ in the neighbourhood of 300, $k$ can be treated as a constant.

### 2.2. *The evaluation of the 'measured' joint p.d.f. and related moments*

The method of analysis involves assuming a certain joint p.d.f. for the three random variables $u$, $v$ and $w$ and finding the transformed joint p.d.f. of $u^*$ and $v^*$, where $u^*$ and $v^*$ are the instantaneous velocities (corresponding to $u$ and $v$, respectively) measured by the X-probe.

For $\alpha = \pm 45°$, we have from (1.2)

$$U_{\mathrm{eff}}(\alpha = 45°) = U_{\mathrm{eff}}(1) = [(u+v)^2 + 2w^2 + k^2(u-v)^2]^{\frac{1}{2}}/2^{\frac{1}{2}},$$
$$U_{\mathrm{eff}}(\alpha = -45°) = U_{\mathrm{eff}}(2) = [(u-v)^2 + 2w^2 + k^2(u+v)^2]^{\frac{1}{2}}/2^{\frac{1}{2}}.$$

The linearizer voltages $E_1$ and $E_2$ will then be directly proportional to $U_{\mathrm{eff}}(1)$ and $U_{\mathrm{eff}}(2)$. Thus

$$\left.\begin{aligned} E_1 &= s_1[(u+v)^2 + 2w^2 + k^2(u-v)^2]^{\frac{1}{2}}/2^{\frac{1}{2}}, \\ E_2 &= s_2[(u-v)^2 + 2w^2 + k^2(u+v)^2]^{\frac{1}{2}}/2^{\frac{1}{2}}. \end{aligned}\right\} \tag{2.8}$$

Assuming that the X-probe is calibrated in a laminar flow ($u' = v' = w' = 0$) in the $u$ direction ($u = U$, $V = W = 0$), as is usually the case, we have during calibration

$$E_i = s_i U(1 + k^2)^{\frac{1}{2}}/2^{\frac{1}{2}} \quad (i = 1, 2).$$

So the slope of the calibration curve of the linearizer voltage *vs.* the component of velocity normal to the hot wire is $s(1 + k^2)^{\frac{1}{2}}$. Then

$$U^*_{\mathrm{eff}}(i) = E_i/\{s_i(1 + k^2)^{\frac{1}{2}}\} \quad (i = 1, 2), \tag{2.9}$$

where the * denotes the velocity inferred by the operator. Henceforth the superscript * will denote the value of a variable measured by the hot-wire anemometer

used in the conventional manner [neglecting rectification, $k$ and higher-order terms in the series expansion of (2.8)]. This conventional technique, in fact, amounts to neglecting $w$ and assuming $U^*_{\text{eff}}$ to be equal to the velocity component normal to the hot wire. Neglecting $k$, $W$ and second-order terms and assuming $V \ll U$, it is easy to show that $[(u+v)^2+2w'^2]^{\frac{1}{2}} \simeq u+v$. From (2.8) and (2.9) we then have

$$\left.\begin{aligned} 2^{\frac{1}{2}}U^*_{\text{eff}}(1) &= u^*+v^* = [(u+v)^2+2w^2+k^2(u-v)^2]^{\frac{1}{2}}/(1+k^2)^{\frac{1}{2}}, \\ 2^{\frac{1}{2}}U^*_{\text{eff}}(2) &= u^*-v^* = [(u-v)^2+2w^2+k^2(u+v)^2]^{\frac{1}{2}}/(1+k^2)^{\frac{1}{2}}. \end{aligned}\right\} \tag{2.10}$$

These equations then give us the transformation from the real $(u, v, w)$ space to the measured $(u^*, v^*)$ plane.

Given $F(u, v, w)$, the joint p.d.f. of the three velocity components, the problem is to find the joint p.d.f. $p(u^*, v^*)$. Consider the transformation

$$\left.\begin{aligned} x = u+v, \quad y = u-v, \quad z = w, \\ x^* = u^*+v^*, \quad y^* = u^*-v^*, \quad z^* = z. \end{aligned}\right\} \tag{2.11}$$

The absolute value of the Jacobian of the transformation being 2, the joint p.d.f. $f(x, y, z)$ is given by

$$f(x, y, z) = \tfrac{1}{2}F[\tfrac{1}{2}(x+y), \tfrac{1}{2}(x-y), z], \tag{2.12}$$

and (2.10) become

$$\left.\begin{aligned} x^* &= (x^2+2z^2+k^2y^2)^{\frac{1}{2}}/(1+k^2)^{\frac{1}{2}}, \\ y^* &= (y^2+2z^2+k^2x^2)^{\frac{1}{2}}/(1+k^2)^{\frac{1}{2}}. \end{aligned}\right\} \tag{2.13}$$

The relations (2.5) then become

$$x^* \geqslant ky^*, \quad y^* \geqslant kx^*.$$

For the transformation $(x, y, z) \rightarrow (x^*, y^*, z)$ given by (2.13) the Jacobian $J$ is given by

$$J = xy(1-k^2)/\{x^*y^*(1+k^2)\}.$$

For a given point $(x^*, y^*, z)$, (2.13) have four roots $(x_i, y_i, z)$ $(i = 1\text{–}4)$. The joint p.d.f. $P(x^*, y^*, z)$ is then given by

$$P(x^*, y^*, z) = \sum_{i=1}^{4} \frac{f(x_i, y_i, z)}{|J_i|} \tag{2.14}$$

and

$$g(x^*, y^*) = \int_{-\infty}^{+\infty} P(x^*, y^*, z)\, dz = \int_{-\omega_0}^{\omega_0} P(x^*, y^*, z)\, dz, \tag{2.15}$$

where $\omega_0$ is a positive number such that for a given $(x^*, y^*)$ equations (2.13) have roots only in the domain $-\omega_0 \leqslant z \leqslant \omega_0$. Obviously, if for a given point $(x^*, y^*, z)$ equations (2.13) have no roots, $P(x^*, y^*, z) = 0$. To find $\omega_0$ rewrite (2.13) as

$$(1-k^4)x^2+2(1-k^2)z^2 = (1+k^2)(x^{*2}-k^2y^{*2}),$$

$$(1-k^4)y^2+2(1-k^2)z^2 = (1+k^2)(y^{*2}-k^2x^{*2}),$$

which represent two orthogonal elliptic cylinders; $\omega_0$ is then clearly given by

$$\omega_0^2 = \min\{(1+k^2)(x^{*2}-k^2y^{*2})/[2(1-k^2)], (1+k^2)(y^{*2}-k^2x^{*2})/[2(1-k^2)]\}.$$

Transforming back to $(u^*, v^*)$ gives $p(u^*, v^*)$. Since $u^* = \frac{1}{2}(x^* + y^*)$ and $v^* = \frac{1}{2}(x^* - y^*)$ the Jacobian is $-\frac{1}{2}$. Thus

$$p(u^*, v^*) = 2g(u^* + v^*, u^* - v^*). \tag{2.16}$$

So, given $F(u, v, w)$, (2.12)–(2.16) yield $p(u^*, v^*)$. The various 'measured' moments and the marginal densities can then be calculated as

$$p_u(u^*) = \int_{-\infty}^{+\infty} p(u^*, v^*)\, dv^*, \quad p_v(v^*) = \int_{-\infty}^{+\infty} p(u^*, v^*)\, du^*,$$

$$\overline{(u^* - U^*)^m (v^* - V^*)^n} = \iint_{-\infty}^{+\infty} (u^* - U^*)^m (v^* - V^*)^n p(u^*, v^*)\, du^*\, dv^*.$$

### 2.3. *Computations*

The computations were performed for the common case in which $\overline{u'w'} = \overline{v'w'} = 0$; as is found, for instance, in two-dimensional and axisymmetric flows. Since $W$ is zero and $V$ is usually very small in such flows, both were chosen to be zero. For simplicity in the computations, it was also assumed that $u$, $v$ and $w$ were jointly normal. Thus

$$F(u, v, w) = \frac{1}{\sigma_u \sigma_v \sigma_w [(2\pi)^3 (1 - \rho^2)]^{\frac{1}{2}}} \times \exp\left[ -\frac{1}{2(1-\rho^2)} \left\{ \frac{(u-U)^2}{\sigma_u^2} + \frac{v^2}{\sigma_v^2} + \frac{w^2}{\sigma_w^2} (1 - \rho^2) - 2\rho \frac{(u-U)v}{\sigma_u \sigma_v} \right\} \right],$$

where $\sigma_u$, $\sigma_v$ and $\sigma_w$ are the standard deviations of $u$, $v$ and $w$ respectively and $\rho$ is the correlation coefficient of $u$ and $v$ $[\rho = \overline{u'v'}/(\sigma_u \sigma_v)]$.

An effective† grid size of $80 \times 160$ was chosen in the $u^*$, $v^*$ plane for computations; a grid twice as coarse gave results differing by less than 1%. Because $F(u, v, w)$ was an exponential function, the integration in (2.15) was very time consuming. With the present grid size the transformation $F(u, v, w) \rightarrow p(u^*, v^*)$ took about 25 min of CPU time on an IBM 370.

To calculate various integrals Simpson's rule was used. The volume under $p(u^*, v^*)$ did not differ from unity by more than 0·005 in any run; it was however normalized to unity after the computations.

The conventional 'measured' correlation between $u'$ and $v'$ is $\overline{u^{*\prime} v^{*\prime}}$, where $u^* = U^* + u^{*\prime}$ and $v^* = V^* + v^{*\prime}$. It can be corrected to some extent. Squaring and subtracting equations (2.10) we have

$$(U^* + u^{*\prime})(V^* + v^{*\prime})(1 + k^2) = (U + u')(V + v')(1 - k^2),$$

taking the average of which gives

$$\overline{u'v'} = U^* V^* (1 + k^2)/(1 - k^2) - UV + \overline{u^{*\prime} v^{*\prime}} (1 + k^2)/(1 - k^2). \tag{2.17}$$

Thus if the real mean transverse component $V$ is zero, which will be the case at the centre-line of an axisymmetric flow, $\overline{u'v'}$ can be measured exactly using (2.17).

† Taking advantage of the fact that the points in the $u^*$, $v^*$ plane are bounded within a sector of included angle $\theta$, the same information could be stored in an $80 \times 80$ matrix.

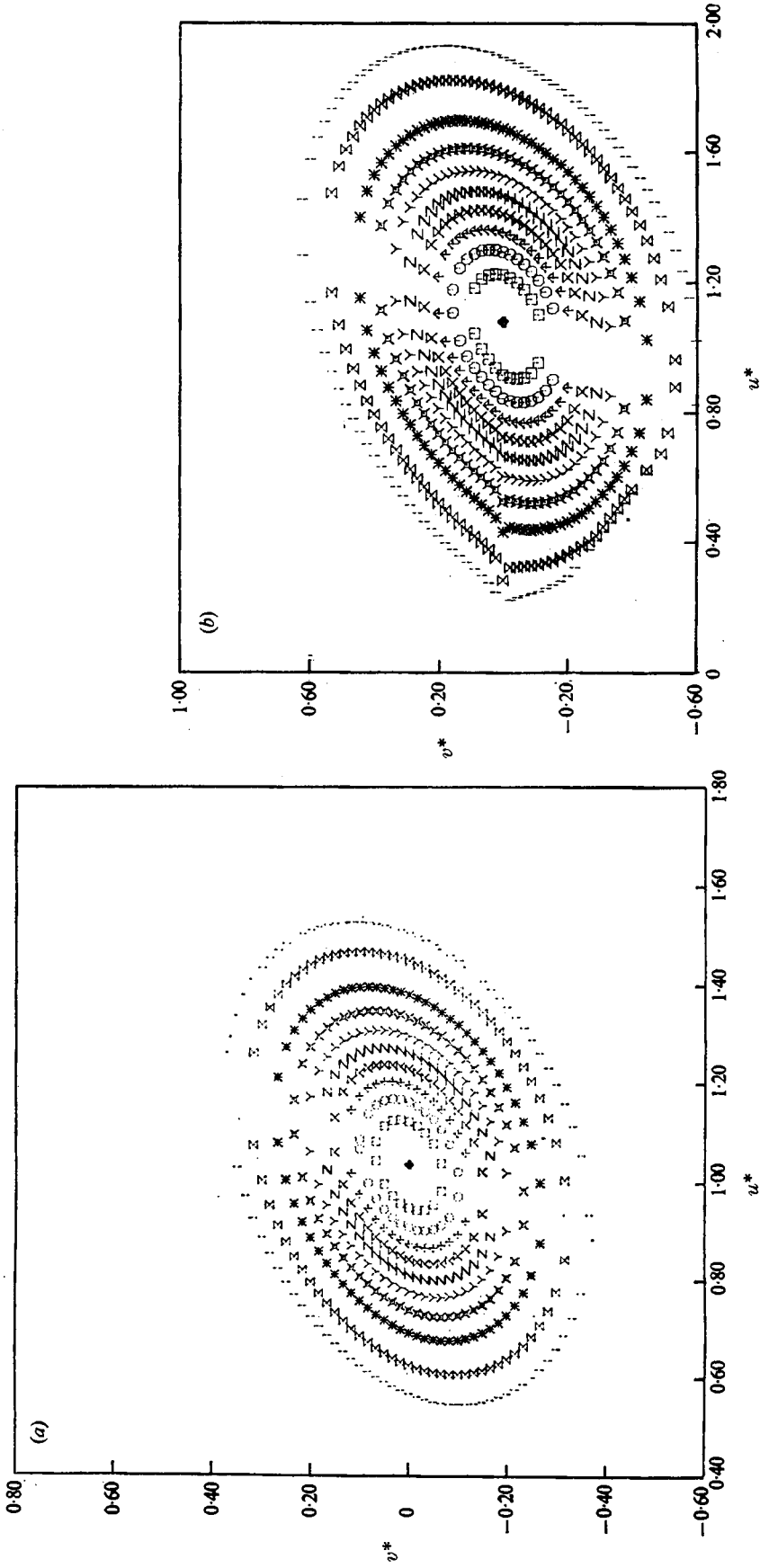


FIGURES 4 (*a*, *b*). For legend see facing page.

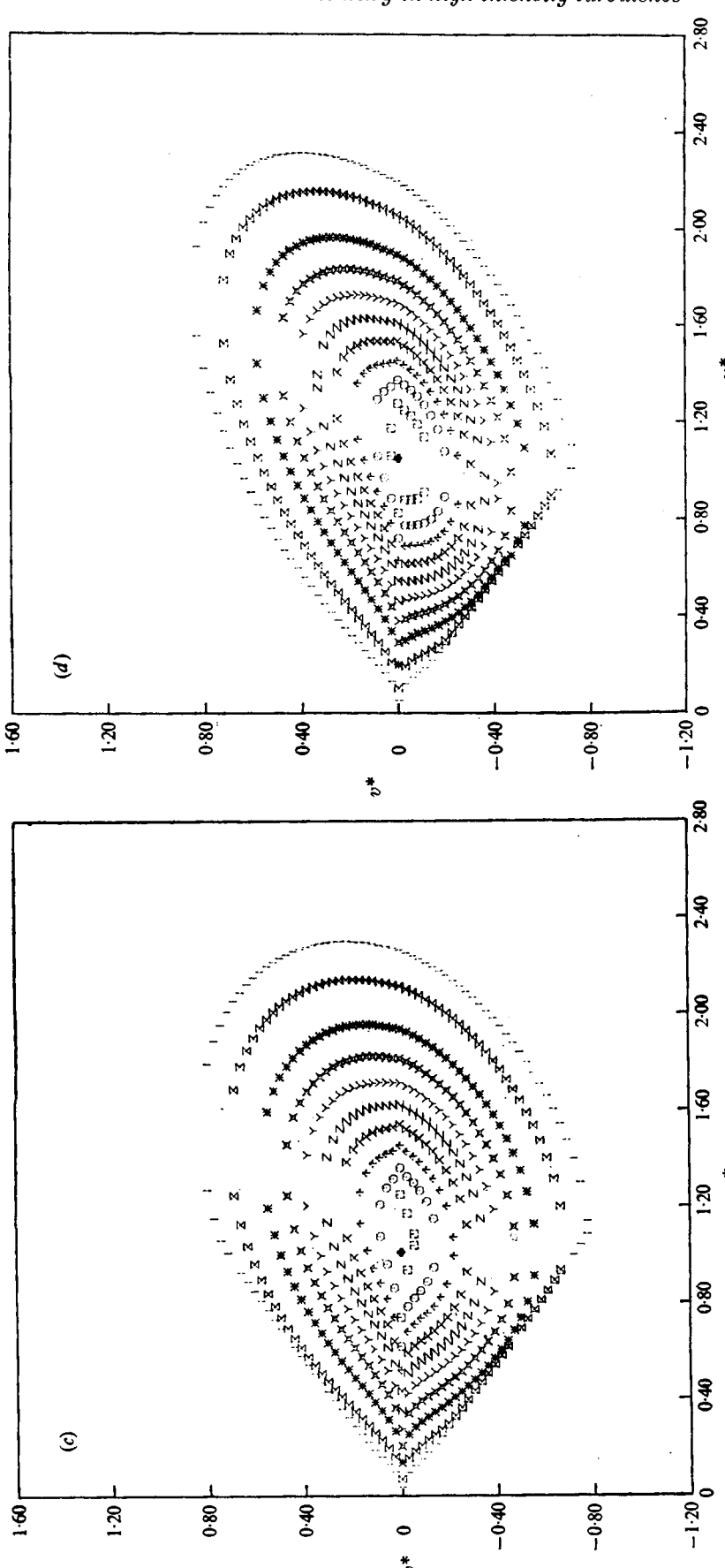


FIGURE 4. Isoprobability contours for $k = 0{\cdot}15$, $\sigma_v = \sigma_w = 0{\cdot}8\sigma_u$, $U = 1$, $V = 0$. |, $p/p_m = 0{\cdot}05$; ⧖, $p/p_m = 0{\cdot}1$; *, $p/p_m = 0{\cdot}2$; ⧖, $p/p_m = 0{\cdot}3$; Y, $p/p_m = 0{\cdot}4$; Z, $p/p_m = 0{\cdot}5$; ⧗, $p/p_m = 0{\cdot}6$; ⧗, $p/p_m = 0{\cdot}7$; O, $p/p_m = 0{\cdot}8$; □, $p/p_m = 0{\cdot}9$; ◆, $p/p_m = 1{\cdot}0$. $p$ = probability density, $p_m$ = maximum value of $p$. (*a*) $\sigma_u/U = 0{\cdot}2$, $\rho = 0{\cdot}3$. (*b*) $\sigma_u/U = 0{\cdot}35$, $\rho = 0{\cdot}3$. (*c*) $\sigma_u/U = 0{\cdot}5$, $\rho = 0{\cdot}3$. (*d*) $\sigma_u/U = 0{\cdot}5$, $\rho = 0{\cdot}5$.

However, that is not always the case. Applying the corrections for $k$ suggested by Champagne & Sleicher (1967), the corrected value of the correlation is equal to the last term in (2.17). Thus the error in the conventional value of $\overline{u'v'}$ is

$$-U^*V^*(1+k^2)/(1-k^2)+UV. \tag{2.18}$$

Therefore, if $V$ were neglected in the original formulation, as was done by Rodi (1971), the error term would still be $UV$, which is at least of the same order as (2.18). Since $U$ and $V$ are not known, $U^*$ and $V^*$ are the best estimates for them. Thus the corrected correlation is

$$(\overline{u'v'})_c = 2k^2U^*V^*/(1-k^2)+\overline{u^{*\prime}v^{*\prime}}(1+k^2)/(1-k^2). \tag{2.19}$$

## 3. Results and discussion

Along the bounds $x^* = ky^*$ and $y^* = kx^*$ in the $x^*$, $y^*$ phase plane, the probability density vanishes because $\omega_0$, and hence the integral (2.15), is zero. An examination of the equiprobability contours in figures 4(*c*) and (*d*) shows that the probability density is quite small for points close to the bounds. This is the reason why the bounds in figure 1 are not sharp, thus requiring several photographs to determine $\theta$ as mentioned in § 2.1.

Because $F(u, v, w)$ has been assumed joint normal, the actual isoprobability contours in the $u$, $v$ plane are a family of ellipses. Figure 4(*a*) shows that for $\sigma_u/U = 0{\cdot}2$ the measured isoprobability contours show very little distortion. Superposition of the actual isoprobability contours for this case revealed only a small translation (to the right) and only a little compression. For higher intensities of turbulence, however, as can be seen in figures 4(*b*)–(*d*), the distortion is quite apparent. (Notice the sharp edge along $v^* = 0$.) The 'bounds' as defined in figure 3, when mapped into the $u^*$, $v^*$ plane, become two vertical (i.e. normal to the $u^*$, $v^*$ plane) planes intersecting at the origin and symmetrically placed about the $u^*$ axis at angles of $\pm(\frac{1}{4}\pi - \tan^{-1}k)$. Thus when the turbulence intensity is increased the joint p.d.f. surface is squeezed and displaced to the right owing to the constraints imposed by the two aforementioned planes. This, however, is not the only reason for distortion since the sensitivity to the $w$ component of velocity plays an equally important role. For low turbulence intensities, as can be seen from figure 5, the effect of the bounds is felt only by the tails of the p.d.f.

In figures 6(*a*) and (*b*) the measured marginal densities of $u^*$ and $v^*$ (for the case $\sigma_u/U = 0{\cdot}5$) are compared with the actual ones, which are normal. Their skewness and flatness factors are plotted in figure 7 as functions of $\sigma_u/U$. It may be noted that the measured skewness of $u^*$ and $v^*$ is always positive† rather than having the real value of zero. Thus the distortions tend to increase (algebraically) the skewness. Consequently, an observed (measured) negative skewness will be a real feature of the flow being investigated.

† If $\rho$ is negative, the skewness of $v^*$ is also negative. This becomes clear on noting that the joint p.d.f. surface $F(u, v, w)$ remains the same for this case (provided that $V = 0$) if the $v$ axis is rotated through $\pi$ rad.

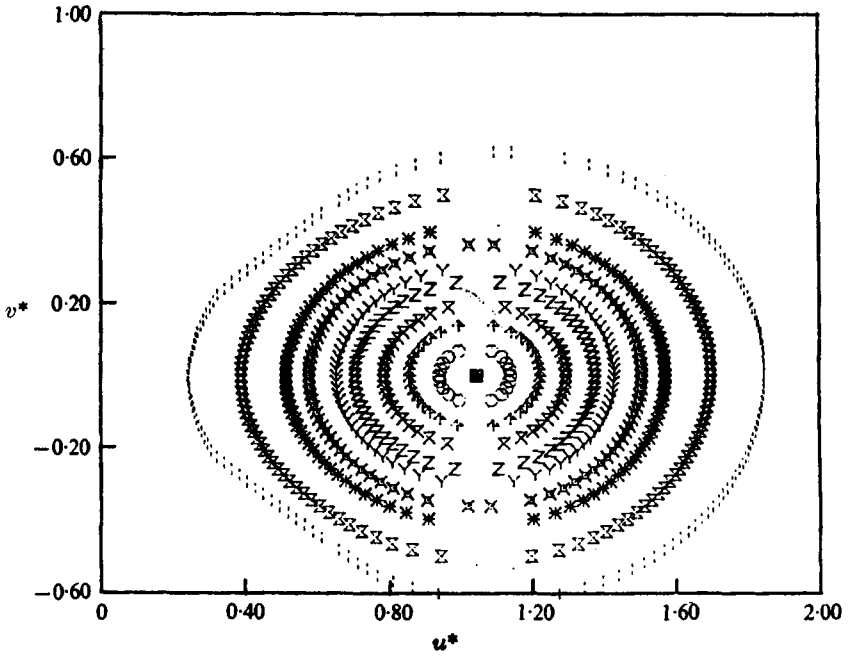


FIGURE 5. Isoprobability contours for $k = 0{\cdot}15$, $\sigma_u/U = 0{\cdot}215$, $\sigma_v/U = \sigma_w/U = 0{\cdot}18$, $\rho = 0{\cdot}01$, $U = 1$, $V = 0$. |, $p/p_m = 0{\cdot}001$; X, $p/p_m = 0{\cdot}01$; *, $p/p_m = 0{\cdot}05$; ⊡, $p/p_m = 0{\cdot}1$; Y, $p/p_m = 0{\cdot}2$; Z, $p/p_m = 0{\cdot}3$; X, $p/p_m = 0{\cdot}5$; ⊕, $p/p_m = 0{\cdot}7$; ○, $p/p_m = 0{\cdot}9$; ⊕, $p/p_m = 1{\cdot}0$.

Further results of the computations are given in table 1 and figure 8. Since the measured correlation $\overline{u^{*\prime}v^{*\prime}}$ was corrected to $(\overline{u'v'})_c$ using (2.19) (which includes the correction due to the sensitivity $k$ described by Champagne & Sleicher 1967), to first order the error in it should be insensitive to $k$. Furthermore, according to Champagne & Sleicher (1967) there is no error in the measured value of $\sigma_u$ (for small turbulence intensities) due to the effect of $k$. This agrees with the results in table 1, which show that the errors in $\sigma_{u^*}$ and $(\overline{u'v'})_c$ are not very sensitive to $k$. Also, the difference between the errors in $\sigma_{v^*}$ for the two cases $k = 0$ and $0{\cdot}15$ agrees fairly well with the correction given by Champagne & Sleicher. It should now be emphasized that for $(\overline{u'v'})_c$ and $\rho^*$, which is equal to $(\overline{u'v'})_c/(\sigma_{u^*}\sigma_{v^*})$, the errors given in various tables and figures are over and above the errors described by Champagne & Sleicher. Table 1 also shows that the errors in various moments are not very sensitive to the correlation coefficient $\rho$. A few computations done for $\rho = 0{\cdot}9$ and $0{\cdot}1$ support this contention. For turbulence intensities below 20 % the errors are reasonably small but above 30 % they can be large, especially for $(\overline{u'v'})_c$. As a rule, the mean velocity is always overestimated and all the second-order moments are underestimated. Consequently, any second-order moment non-dimensionalized with the local mean velocity will show an even greater error. The error in $\sigma_{v^*}$ is almost twice that for $\sigma_{u^*}$. Because both $\sigma_{u^*}$ and $\sigma_{v^*}$ are underestimated, the error in $\rho^*$ is less than that for $(\overline{u'v'})_c$.

To find out the relative importance of rectification and the $w$ component of velocity, computations were carried out for the case of pure rectification

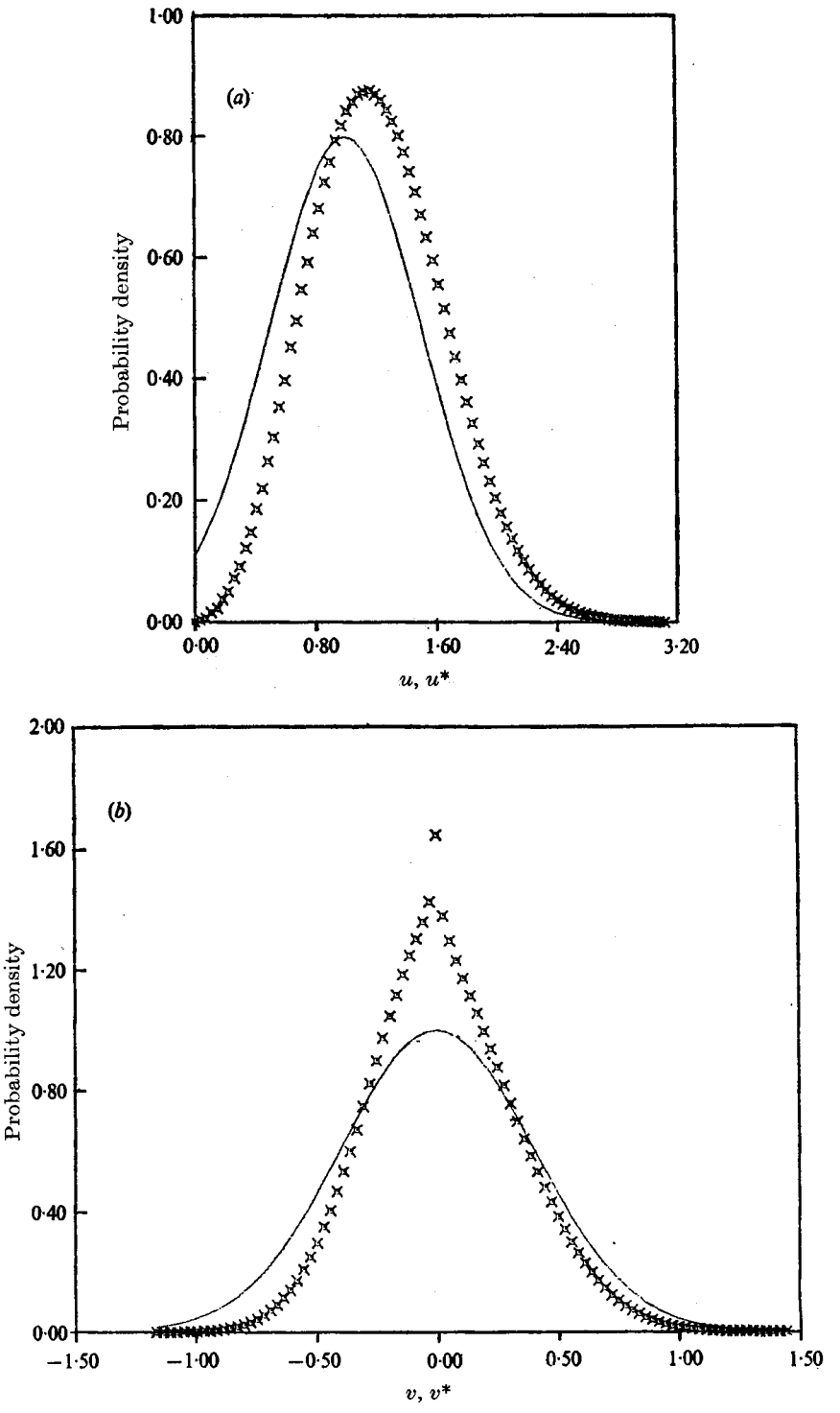


FIGURE 6. Marginal p.d.f. of (*a*) $u$ and $u^*$ and (*b*) $v$ and $v^*$ for $k = 0{\cdot}15$, $\sigma_u/U = 0{\cdot}5$, $\sigma_v = \sigma_w = 0{\cdot}8\sigma_u$, $\rho = 0{\cdot}3$, $U = 1$, $V = 0$. ——, the actual p.d.f.; ⌑, the measured p.d.f. Negative portion of the actual p.d.f. not shown.

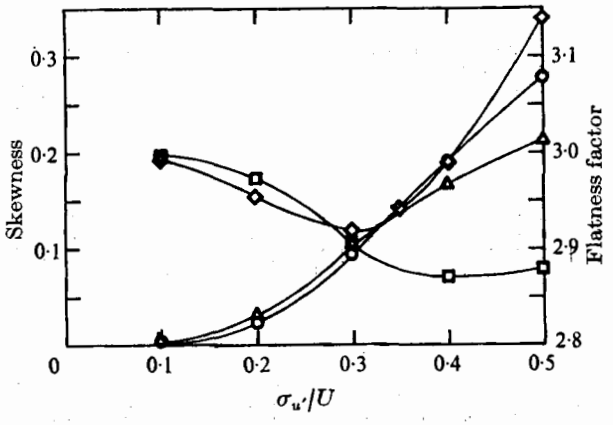


FIGURE 7. Skewness $\overline{(u^{*\prime 3}}/\overline{(u^{*\prime 2})^{\frac{3}{2}}}$ for $u^*$) and flatness factors $\overline{(u^{*\prime 4}}/\overline{(u^{*\prime 2})^2}$ for $u^*$) as functions of turbulence intensity. $k = 0{\cdot}15, \rho = 0{\cdot}3, \sigma_v = \sigma_w = 0{\cdot}8\sigma_u, V = 0{\cdot}0$. ◇, flatness factor of $v^*$; △, skewness of $v^*$; □, flatness factor of $u^*$; ○, skewness of $u^*$. Skewness and flatness factors for $u$ (and also for $v$) are zero and 3·0, respectively.

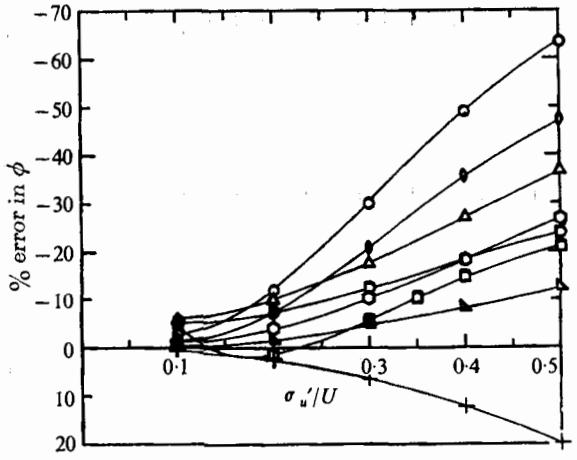


FIGURE 8. Errors as functions of turbulence intensity. $k = 0{\cdot}15, \rho = 0{\cdot}3, \sigma_v = \sigma_w = 0{\cdot}8\sigma_u$. ○, $\phi = \overline{(u'v')_c}/U^{*2}$; ●, $\phi = \overline{(u'v')_c}$; △, $\phi = \sigma_{v^*}/U^*$; ●, $\phi = \sigma_{u^*}/U^*$; ■, $\phi = \sigma_{v^*}$; □, $\phi = \rho^*$; ▲, $\phi = \sigma_{u^*}$; +, $\phi = U^*$.

($k = W = \sigma_w = 0$). The results, together with some of those from table 1, are shown in table 2. As expected, for low turbulence intensities the errors due to rectification are small; for higher intensities, however, they become comparable to those due to the $w$ component. The errors in $\overline{(u'v')_c}/U^{*2}$ due to these two causes become almost the same for $\sigma_u/U \simeq 0{\cdot}4$. Thus the importance of rectification is quite clear, and it should be noted at this point that the errors due to these two effects are of the same sign and augment each other.

Because rectification will occur earlier with an inclined wire compared with a single wire held normal to the mean flow, the error in $\sigma_{u^*}$ as measured by a single wire should be less. This is indeed so, as can be seen from the results shown in table 3 for the case $k = 0$.

| | $\sigma_u/U$ | % error in $U^*$ | % error in $\sigma_{u^*}/U^*$ | % error in $\sigma_{v^*}/U^*$ | % error in $(\overline{u'v'})_c/U^{*2}$ | % error in $\rho^*$ | % error in $(\overline{u'v'})_c$ | % error in $\sigma_{u^*}$ | % error in $\sigma_{v^*}$ |
|---|---|---|---|---|---|---|---|---|---|
| $k = 0{\cdot}0$ | 0·1 | 0·6 | −0·9 | −1·3 | −2·6 | −0·5 | −1·3 | −0·3 | −0·7 |
| | 0·2 | 2·6 | −3·8 | −5·4 | −11·4 | −2·7 | −6·6 | −1·2 | −2·9 |
| | 0·3 | 6·3 | −9·5 | −12·9 | −29·4 | −10·4 | −20·1 | −3·8 | −7·4 |
| $\rho = 0{\cdot}3$ | 0·4 | 12·0 | −17·6 | −22·6 | −49·4 | −20·6 | −36·5 | −7·7 | −13·4 |
| | 0·5 | 19·5 | −26·1 | −32·3 | −64·2 | −28·5 | −48·9 | −11·7 | −19·1 |
| $k = 0{\cdot}15$ | 0·1 | 0·7 | −0·9 | −5·7 | −2·7 | −4·2 | −1·4 | −0·3 | −5·1 |
| | 0·2 | 2·7 | −4·0 | −9·9 | −11·9 | +1·8 | −7·1 | −1·4 | −7·4 |
| | 0·3 | 6·5 | −10·0 | −17·5 | −29·9 | −5·6 | −20·5 | −4·2 | −12·2 |
| $\rho = 0{\cdot}3$ | 0·4 | 12·3 | −18·1 | −27·0 | −48·9 | −14·5 | −35·6 | −8·1 | −18·1 |
| | 0·5 | 19·9 | −26·7 | −36·5 | −63·2 | −20·8 | −47·1 | −12·0 | −23·9 |
| $k = 0{\cdot}0$ | 0·1 | 0·6 | −0·9 | −1·3 | −2·6 | −0·4 | −1·4 | −0·3 | −0·7 |
| | 0·2 | 2·7 | −3·9 | −5·5 | −11·5 | −2·5 | −6·7 | −1·3 | −3·0 |
| | 0·3 | 6·4 | −10·2 | −13·7 | −29·6 | −9·1 | −20·2 | −4·5 | −8·2 |
| $\rho = 0{\cdot}5$ | 0·4 | 12·2 | −18·6 | −23·9 | −49·2 | −18·0 | −36·0 | −8·7 | −14·6 |
| | 0·5 | 19·8 | −27·0 | −33·4 | −63·9 | −25·6 | −48·2 | −12·6 | −20·3 |
| $k = 0{\cdot}15$ | 0·1 | 0·7 | −1·0 | −5·7 | −2·7 | +4·2 | −1·5 | −0·3 | −5·1 |
| | 0·2 | 2·7 | −4·2 | −10·1 | −12·2 | +2·1 | −7·3 | −1·6 | −7·7 |
| | 0·3 | 6·6 | −10·7 | −18·3 | −30·0 | −4·1 | −20·5 | −4·8 | −12·9 |
| $\rho = 0{\cdot}5$ | 0·4 | 12·5 | −19·1 | −28·1 | −48·7 | −11·8 | −35·1 | −9·0 | −19·1 |
| | 0·5 | 20·2 | −27·6 | −37·4 | −62·8 | −18·0 | −46·4 | −13·0 | −24·8 |

TABLE 1. Errors in measurements with an X-probe. $\sigma_v = \sigma_w = 0{\cdot}8\sigma_u$, $\overline{u'w'} = \overline{v'w'} = 0$, error = 'measured' value − actual value

| | % error in $U^*$ | | % error in $\sigma_{u^*}/U^*$ | | % error in $\sigma_{v^*}/U^*$ | | % error in $(u'v')_c/U^{*2}$ | | % error in $\rho^*$ | |
|---|---|---|---|---|---|---|---|---|---|---|
| $\sigma_u/U$ | 1 | 2 | 1 | 2 | 1 | 2 | 1 | 2 | 1 | 2 |
| 0·2 | 2·6 | 0·0 | −3·8 | −0·1 | −5·4 | −0·0 | −11·4 | −0·3 | −2·7 | −0·2 |
| 0·3 | 6·3 | 0·2 | −9·5 | −1·5 | −12·9 | −1·4 | −29·4 | −8·0 | −10·4 | −5·3 |
| 0·4 | 12·0 | 1·2 | −17·6 | −6·1 | −22·6 | −5·6 | −49·4 | −25·4 | −20·6 | −15·8 |
| 0·5 | 19·5 | 3·6 | −26·1 | −12·9 | −32·3 | −11·8 | −64·2 | −42·1 | −28·5 | −24·6 |

TABLE 2. Relative importance of rectification and the $w$ component of velocity. Case 1: $k = 0$, $\sigma_v = \sigma_w = 0{\cdot}8\sigma_u$, errors due to combined effects of rectification and sensitivity to $w$ component. Case 2: pure rectification, $k = W = \sigma_w = 0$, $\sigma_v = 0{\cdot}8\sigma_u$, $\rho = 0{\cdot}3$.

| $\sigma_u/U$ | % error in $U^*$ | % error in $\sigma_{u^*}/U^*$ | % error in $\sigma_{u^*}$ |
|---|---|---|---|
| 0·1 | 0·32 | −0·56 | −0·24 |
| 0·2 | 1·3 | −2·2 | −0·95 |
| 0·3 | 3·0 | −5·3 | −2·4 |
| 0·4 | 5·7 | −10·3 | −5·1 |
| 0·5 | 9·6 | −16·8 | −8·8 |

TABLE 3. Errors in measurements with a single wire in the $u$, $v$ plane held normal to the $u$ direction. $W = 0$, $\overline{u'w'} = 0$, $\sigma_w = 0{\cdot}8\sigma_u$, $k = 0$.

It should be remembered that the above errors were calculated assuming an initial joint normal p.d.f. in $u$, $v$, $w$ space and the actual errors in measurement would depend upon the p.d.f. in the flow under investigation. If the actual joint p.d.f. in the flow were skewed in the proper direction, it is possible that the computed errors (for the same $\sigma_u/U$) could be less. Therefore, to estimate the errors in the intermittent region of the flow a weighted (with the intermittency factor) sum of the turbulence intensities in the turbulent and non-turbulent regions should be used. Since the inverse transformation $p(u^*, v^*) \rightarrow F(u, v, w)$ is multi-valued, it is not possible to find the actual p.d.f. and moments given the measured ones. Nevertheless, the analysis provides an estimate of the errors involved.

## 4. Concluding remarks

In high intensity turbulent flows, the axial sensitivity $k$, the sensitivity to the $w$ component of velocity and rectification are the three sources of errors in conventional measurements with cross-wires. Champagne & Sleicher (1967) have demonstrated that the error in second-order moments due to $k$ is negative. It has been shown here that the errors due to the other two causes (independently) are of the same sign. The sensitivity to the $w$ component of velocity and rectification severely distort the joint p.d.f. surface (in the $u^*$, $v^*$ plane), which is confined within a certain sector. Thus care is needed in interpreting the p.d.f. data measured in high intensity turbulent flows. For turbulence intensities greater than 30 %, an X-probe can lead to results with significantly large errors, the error

in $(\overline{u'v'})_c$ being 28 % (over and above the error due to the influence of $k$ given by Champagne & Sleicher) when the turbulence intensity is 35 %.

The authors gratefully acknowledge the financial assistance of the National Science Foundation under Grants GK-30479 and GK-21214.

## REFERENCES

CHAMPAGNE, F. H. & SLEICHER, C. A. 1967 *J. Fluid Mech.* **28**, 177.
CHAMPAGNE, F. H., SLEICHER, C. A. & WEHRMANN, O. H. 1967 *J. Fluid Mech.* **28**, 153.
ECKELMANN, H. 1974 *J. Fluid Mech.* **65**, 439.
HESKESTAD, G. 1965 *J. Appl. Mech.* **32**, 721.
RODI, W. 1971 *Imperial College, Dept. Mech. Engng Rep.* ET/TN/B/10.
WYGNANSKI, I. & FIEDLER, H. 1969 *J. Fluid Mech.* **38**, 577.

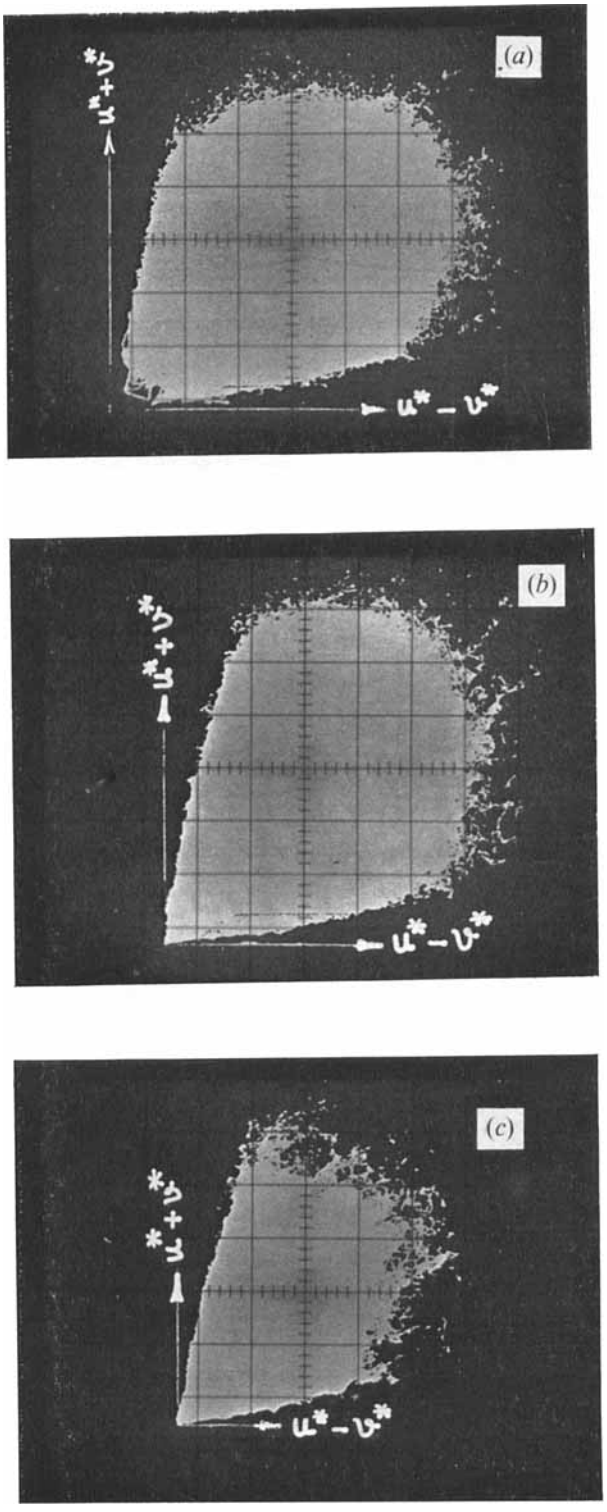


FIGURE 1. Phase diagrams for linearized signals from two orthogonal hot wires (placed at $\pm 45^\circ$ to the longitudinal direction) in an axisymmetric turbulent jet of air 15 diameters downstream. (*a*) Approximately at the centre-line of the jet; $\sigma_{u^*}/U^* = 0{\cdot}21$, $\sigma_{v^*}/U^* = 0{\cdot}17$, $\rho^* = -0{\cdot}08$. (*b*) Point of maximum shear $r/r_{\frac{1}{2}} = 0{\cdot}73$; $\sigma_{u^*}/U^* = 0{\cdot}32$, $\sigma_{v^*}/U^* = 0{\cdot}22$, $\rho^* = 0{\cdot}34$. (*c*) Intermittency factor $\approx 0{\cdot}6$; $\sigma_{u^*}/U^* = 0{\cdot}59$, $\sigma_{v^*}/U^* = 0{\cdot}29$, $\rho^* = 0{\cdot}29$.